

SLAC-PUB-7665
October 1997

Ion Effects in the SLC Electron Damping Ring under Exceptionally Poor Vacuum Conditions*

Frank Zimmermann, Patrick Krejcik, Michiko Minty, David Pritchau,
Tor Raubenheimer, Marc Ross, Mark Woodley
Stanford Linear Accelerator Center, Stanford University, CA 94309

In 1996, due to a catastrophic kicker chamber failure in the SLC electron damping ring, the ring vacuum system was contaminated for several months. During this time, the vertical emittance of the beam extracted from the ring was increased by a large factor (4-20). The emittance slowly decreased as the vacuum pressure gradually improved. At the same time, an intermittent vertical instability was observed. Both the emittance blow-up and the instability behavior depended strongly on beam current, ring pressure, number of bunches in the ring (1 or 2), duty cycle, store time and betatron tunes. In this report, we describe the observations, and compare them with predictions from classical ion-trapping and ion-instability theories.

*Presented at the International Workshop on Multi-Bunch Instabilities
in Future Electron and Positron Accelerators (MBI97),
KEK, Tsukuba, Japan, July 15-18, 1997*

*Work supported by the US Department of Energy under Contract DE-AC03-76SF00515 and by the Tsukuba EXPO'85 Memorial Foundation.

Ion Effects in the SLC Electron Damping Ring under Exceptionally Poor Vacuum Conditions*

Frank Zimmermann, Patrick Krejcik, Michiko Minty, David Pritzkau,
Tor Raubenheimer, Marc Ross, Mark Woodley

Stanford Linear Accelerator Center, Stanford University, CA 94309

Abstract

In 1996, due to a catastrophic kicker chamber failure in the SLC electron damping ring, the ring vacuum system was contaminated for several months. During this time, the vertical emittance of the beam extracted from the ring was increased by a large factor (4–20). The emittance slowly decreased as the vacuum pressure gradually improved. At the same time, an intermittent vertical instability was observed. Both the emittance blow-up and the instability behavior depended strongly on beam current, ring pressure, number of bunches in the ring (1 or 2), duty cycle, store time and betatron tunes. In this report, we describe the observations, and compare them with predictions from classical ion-trapping and ion-instability theories.

1 INTRODUCTION

The two dampings ring of the Stanford Linear Collider (SLC) reduce the initial emittance of 1.19-GeV electron or positron beams by a factor 5–6 horizontally and 100–200 vertically, before the bunches are injected into the SLAC linac and transported to the collision point. The rings nominally operate with a 120-Hz duty cycle, which corresponds to a store time of 8.3 ms for electrons and 16.6 ms for positrons. In each ring, two bunches are stored simultaneously. In the electron ring the bunches are injected into the 1st and 41st rf bucket (the harmonic number is 84), while in the positron ring the bunches are placed exactly diametrically. For study purposes, the rings can also be operated with a single bunch or at a reduced repetition rate (e.g., at 60 Hz). The nominal electron damping-ring parameters are listed in Table 1 and a schematic layout of one of the two rings is depicted in Fig. 1.

In 1996, due to the failure of a kicker vacuum chamber the electron ring vented to atmosphere, and the vacuum system was contaminated by combustion products from magnet insulation. During the following months, the vacuum conditions were unusually poor, with an average pressure around 10^{-7} Torr. The resulting emittance growth and beam instabilities have been reported previously in Ref. [6]. Measurements of transverse beam-transfer-functions under poor vacuum conditions and their possible interpretation were discussed in Ref. [7].

Ion-related effects caused by the poor vacuum considerably limited the 1996 SLC machine performance. Thus,

an understanding of the beam-ion dynamics and the development of possible cures are of great interest for future damping-ring operation. In addition, since only two bunches are stored (the simplest multi-bunch system!) and the circumference is rather small, the electron damping ring is ideally suited for the experimental study of multi-bunch trapped ion effects. Finally, since during the short store time the beam size changes significantly, many of the observed ion effects are transient in nature and may differ from those seen in storage rings with longer store (and injection) times. Such transient ion effects will likely become relevant for the next generation of light sources or colliders [1].

parameter	value
circumference C	35 m
beam energy E	1.19 GeV
initial emittances $\gamma\epsilon_x^i, \gamma\epsilon_y^i$	20×10^{-5} m
final emittances $\gamma\epsilon_x^f, \gamma\epsilon_y^f$	$3, 0.2 \times 10^{-5}$ m
horiz. damping time τ_x [2, 3]	3.3 ± 0.3 ms
vert. damping time τ_y [2, 3]	4.1 ± 0.3 ms
longitudinal damping time τ_s	1.5 ms
store time τ_{store}	8.3 ms
no. of bunches n_b	2
bunch population N_b	$\sim 4 \times 10^{10}$
rf gap voltage V_c	820 kV
rf frequency f_{RF}	714 MHz
revolution frequency f_0	8.5 MHz
harmonic number h	84
momentum compaction α	0.0147
rms bunch length σ_z [4]	6.5 mm
relative energy spread σ_δ	9×10^{-4}
tunes Q_x, Q_y	8.23, 3.42

Table 1: Parameters of the SLC electron damping ring.

2 EMITTANCE AND BEAM LIFETIME

2.1 Observations

The most obvious effect of the poor vacuum was an increase in the vertical beam size of the extracted beam. The blow up was clearly evident on a profile monitor in the ring-to-linac transfer line (RTL), as illustrated in Fig. 2. The figure shows that for the normal store time of 8.3 ms the vertical beam size was much larger when two bunches were stored in the ring than when only a single bunch was stored. This sensitivity to the number of bunches suggests that the

* Work supported by the US Department of Energy under Contract DE-AC03-76SF00515 and by the Tsukuba EXPO'85 Memorial Foundation.

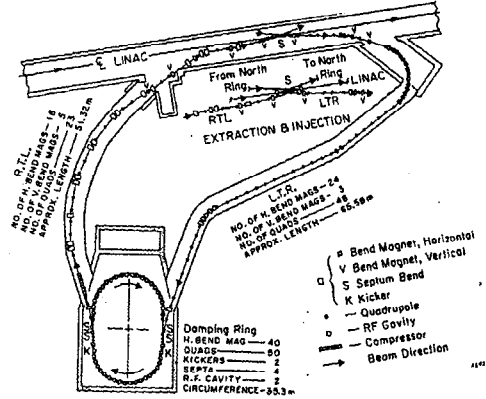


Figure 1: Schematic layout of one of the two SLC damping rings. The beam transfer lines (called LTR and RTL) connecting the ring to the linac are also depicted.

vertical blow-up was caused by (temporarily) trapped ions, which are much more likely to occur for 2 bunches than for a single bunch. A more precise measure of the beam size can be obtained with an RTL wire scanner. Wire-scan results with 1 and 2 bunches, shown in Fig. 3, confirmed the enormous vertical blow-up with two bunches and in addition revealed a very non-Gaussian beam shape. A non-Gaussian shape would be expected as a result of filamentation in the transverse phase space [5], *e.g.*, induced by a collective instability.

Figure 4 presents wire-scan measurements for a 16.6-ms long store time (twice the nominal). In this case the vertical beam size for two bunches and for a single bunch were roughly identical: the two-bunch beam size was about 5 times (!) and the single-bunch beam size still about 30% smaller than the beam sizes obtained for an 8.3-ms store time in Fig. 3. These beam sizes agreed with the values typically achieved at nominal vacuum pressure (10^{-8} Torr) with an 8.3-ms store time. Also, for the 16.6-ms store time, the non-Gaussian tails disappeared (Fig. 4). Based on this experience, comparing the extracted vertical beam sizes for short and long store times has now become a routine diagnostic for detecting possible vacuum problems in the SLC electron damping ring.

Figure 5 illustrates that the extracted vertical beam size was not only very sensitive to the number of bunches and to the store time, but also to the vertical betatron tune. A tune value just below the half integer resonance ($Q_y \approx 3.45$), at which the beam size was relatively small, was chosen as the standard working point. For tunes above the half integer the beam size was significantly larger. This sensitivity to the betatron tune was in strong contrast to the behavior seen under normal vacuum conditions, where the extracted beam size is nearly independent of the tune, disregarding the blow-up on a few very narrowly confined resonances.

It was further observed that the duty cycle of the accelerator had a great impact on the extracted beam emittance. For the same short store time of 8.3 ms, the extracted vertical beam size with a 20 Hz cycle period was significantly

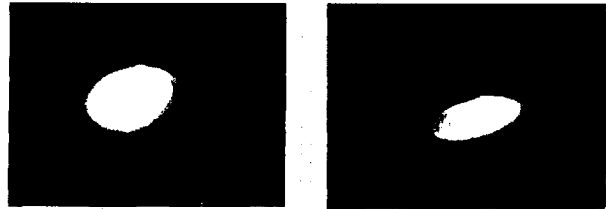


Figure 2: Extracted beam size viewed on a profile monitor in the ring-to-linac transfer line, for a store time of 8.3 ms and operation with two bunches (left) and with a single bunch (right).

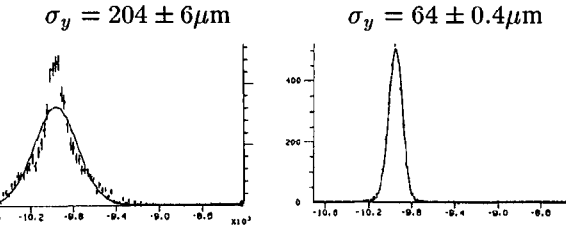


Figure 3: Extracted beam size measured with a wire scanner in the ring-to-linac transfer line, for a store time of 8.3 ms and operation with two bunches (left) and with a single bunch (right). Shown are the counts in a detector versus the wire position in microns. The rms beam size obtained from a Gaussian fit is also given [6].

larger than that observed with the regular 120-Hz repetition rate, although the average pressure was much improved in the former case. The difference in the beam size for 20 and 120 Hz repetition frequencies increased with the beam current. It is not understood why the beam size was so sensitive to the duty cycle. Possible reasons could be a change of magnet positions, magnet fields or the ring circumference due to thermal variation, unrelated to the vacuum, or a local outgassing that was aggravated by the discontinuous 20-Hz operation.

The strong difference in the vertical beam sizes and shapes for short and long store times, and (perhaps) also

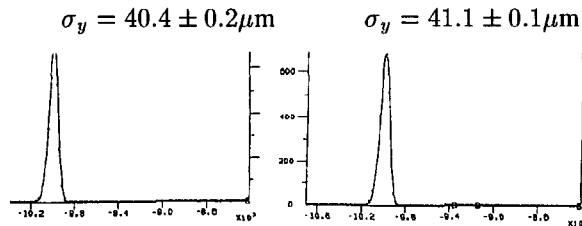


Figure 4: Extracted beam size measured with a wire scanner in the ring-to-linac transfer line, for a store time of 16.6 ms and operation with two bunches (left) and with a single bunch (right). Shown are the counts in a detector versus the wire position in microns. The rms beam size obtained from a Gaussian fit is also given.

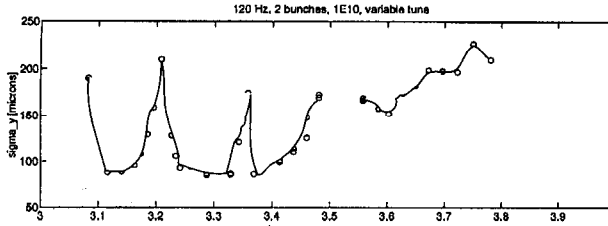


Figure 5: Measured vertical size of the extracted beam as a function of the betatron tune Q_y , for an 8.3-ms store time and 2-bunch operation.

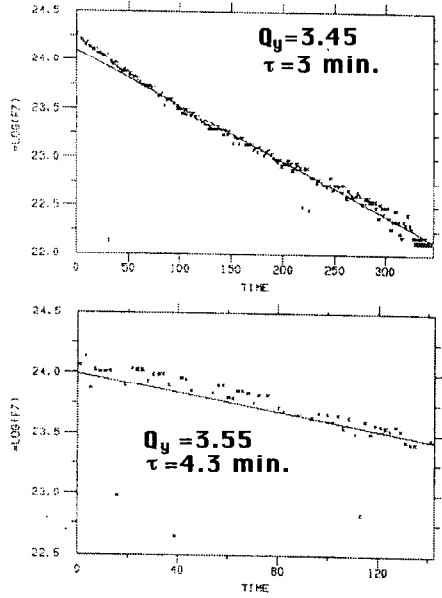


Figure 6: Bunch population versus time after injection for two different betatron tunes Q_y . The vertical coordinate is the natural logarithm of the bunch population, $\ln N_b$; the horizontal coordinate is the time in seconds. The fitted slope gives the exponential beam lifetime, whose value is also shown.

the peculiar dependence of the extracted beam size on the duty cycle, indicate that the ion effects reported so far were mostly transient in nature.

Non-transient ion effects were studied by storing the beam for a much longer period of time (e.g., for several minutes). In this case, the current was seen to decay with a lifetime of about 100–250 s. This was considerably smaller than the beam lifetime observed under nominal vacuum conditions. (The latter is about 8–10 minutes and consistent with the estimated lifetime due to Touschek scattering.) Further, it was observed that the beam lifetime was also sensitive to the betatron tune. Figure 6 illustrates that a vertical betatron tune just above the half integer resonance (3.55) yielded a 40% higher lifetime than a tune just below the half integer (3.45), although, as seen in Fig. 5, the vertical beam size was much smaller in the latter case.

Since for normal operation the beam is stored in the ring only for 8.3 ms, the (much longer) beam lifetime is of no

direct concern.

2.2 Theory

In order to compare the beam observations with theoretical expectations, we now describe under which conditions and at which times after injection ions could be trapped by the beam and we discuss different mechanisms by which ions might reduce the beam lifetime.

2.2.1 Ion Density

When two bunches with a total population of $N_{tot} \approx 8 \times 10^{10}$ electrons are stored in the North damping ring, they ionize the residual gas at a rate

$$\lambda_{ion} \approx 4 \times 10^{11} \text{ m}^{-1} \text{s}^{-1} \frac{p}{100 \text{ nTorr}} \quad (1)$$

where λ_{ion} denotes the longitudinal ion density (in units of m^{-1}) and p the gas pressure, the dot indicates a derivative with respect to time, and, considering carbon monoxide as a typical molecule, we have assumed a collisional-ionization cross section of 2 Mbarn.

The beam size decreases during the store due to radiation damping. The horizontal and vertical beam sizes as a function of time are given by

$$\sigma_x(t) = \sqrt{\epsilon_x(t) \beta_x + \eta_x^2 \sigma_\delta^2(t)} \quad (2)$$

$$\sigma_y(t) = \sqrt{\epsilon_y(t) \beta_y + \eta_y^2 \sigma_\delta^2(t)} \quad (\eta_y \approx 0) \quad (3)$$

where $\beta_{x,y}$ and $\eta_{x,y}$ denote the average beta and dispersion functions, and the emittances and energy spread damp during the store as follows:

$$\epsilon_x(t) = \epsilon_{x,0} e^{-2t/\tau_x} + (1 - e^{-2t/\tau_x}) \epsilon_{x,\infty} \quad (4)$$

$$\epsilon_y(t) = \epsilon_{y,0} e^{-2t/\tau_y} + (1 - e^{-2t/\tau_y}) \epsilon_{y,\infty} \quad (5)$$

$$\sigma_\delta(t) = \sigma_{\delta,0} e^{-t/\tau_\delta} + (1 - e^{-t/\tau_\delta}) \sigma_{\delta,\infty}. \quad (6)$$

Here ϵ_x is the (unnormalized) horizontal emittance, ϵ_y the vertical emittance, σ_δ the rms energy spread, $\tau_x \approx \tau_y$ the transverse damping time, τ_δ the longitudinal damping time, and the subindices '0' and '∞' refer to the initial and equilibrium values, respectively. In the following, we will assume a set of typical values listed in Table 2.

If the beam sizes are large, e.g., directly after injection into the ring, the ions are trapped between bunches and start to accumulate, until the ion density approaches a limiting value determined by either of two different effects: First, the total number of ions cannot exceed the number of beam particles, because of the repelling ion space-charge field [8]. For the SLC damping ring, this 'neutralization' density is about $\lambda_{neutral} \approx 2 \times 10^9 \text{ m}^{-1}$, and, at 100 nTorr, it would be reached after about 6 ms store time (assuming all the produced ions are trapped over this period of time). The second limit on the maximum ion density arises because the cross section for second ionization is about equal to that for first ionization [8]. Doubly ionized atoms are over-focused in the gap between bunches and cannot be trapped by

parameter	value
$\gamma\epsilon_{x0}$	20×10^{-5} m
$\gamma\epsilon_{y0}$	20×10^{-5} m
$\sigma_{\delta,0}$	0.01
$\gamma\epsilon_{x\infty}$	3×10^{-5} m
$\gamma\epsilon_{y\infty}$	0.2×10^{-5} m
$\sigma_{\delta,\infty}$	7×10^{-4}
$\langle \beta_x \rangle$	0.7 m
$\langle \beta_y \rangle$	2.5 m
$\langle \eta_x \rangle$	0.1 m

Table 2: Typical initial and equilibrium emittances, energy spread, and average optical functions for the SLC electron damping ring.

the beam. This implies that under quasi-stationary conditions the maximum density of trapped singly-ionized atoms can never be larger than the residual gas density. For a pressure of 100 nTorr, the latter corresponds to a line density of $\lambda_{max} \approx 1.6 \times 10^9$ m⁻¹ at injection, decreasing to $\lambda_{max} \approx 1.6 \times 10^7$ m⁻¹ at the end of the store (the ion line density changes because of the decreasing transverse beam size, while both the gas and the ion density are taken to be constant during the store).

Figure 7 illustrates the expected evolution of the ion density as a function of time after injection. The ions accumulate, until their volume density equals the density of the residual gas, at which point the number of ions and also the ion line density start to decrease, due to the shrinking beam emittance. Thus, in the SLC electron damping ring

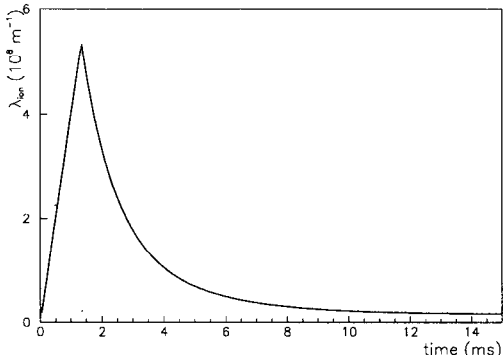


Figure 7: Predicted ion line density (in 10^8 m⁻¹) as a function of time during the store, for an average carbon-monoxide pressure of 100 nTorr.

the ion line density is always much smaller than the neutralization density $\lambda_{neutral}$, and the number of ions is determined solely by the density of the residual gas and the transverse beam size.

2.2.2 Ion Trapping

A single ion is trapped by the beam, if its mass exceeds the critical mass, which, in units of the proton mass, is given

by [8]:

$$A_{crit}(t) = \frac{N_{tot}Cr_pQ}{n_b^2 2\sigma_y(t)(\sigma_x(t) + \sigma_y(t))} \quad (7)$$

where C is the ring circumference, r_p the classical proton radius, Q the ion charge (in units of e), n_b the number of bunches, and σ_x (σ_y) the horizontal (vertical) rms beam size. In principle, the trapping condition is modified by the ion-cloud space-charge field [8]. However, for ion densities much below the neutralization density, as it is the case here, this effect can be neglected. Since the emittances decrease after injection, the critical ion mass is a function of time. This is illustrated for a single bunch and for two bunches by the two curves in Fig. 8, where we assumed typical values for the (initial and final) emittances and the beam energy spread as given in Table 2. The figure shows that different ion species become overfocused in the interbunch gap and get lost at different times during the store, e.g., hydrogen ions are lost after about 1.3 ms and carbon monoxide ions after 6 ms. At the time when the ions become unstable, the ion cloud may coherently interact with the beam. This in turn can blow up the beam emittance and re-stabilize the ions, which may explain repeated strong excitations of betatron motion which were observed at various times during the store (see later).

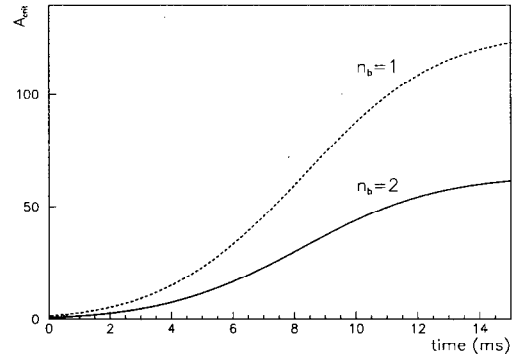


Figure 8: Predicted critical ion mass (in units of proton mass) as a function of time during the store, comparing operation with 1 or 2 bunches. Ions with $A > A_{crit}$ are trapped by the beam.

For single-bunch operation, a betatron tune shift indicating the trapping of ions was observed when the bunch population decayed below about 1.5×10^{10} (see Fig. 9). Evaluating Eq. (7) at this threshold current, we find an ion mass of about 40–50, which would be consistent with carbon dioxide molecules.

2.2.3 Beam lifetime

Ions trapped in the beam can reduce the beam lifetime by a variety of effects: (1) bremsstrahlung in the field of the atomic (or ionic) nuclei, (2) single Coulomb scattering outside of the acceptance, (3) excitation by ion-driven collec-

tive instabilities, or (4) changes to the single particle dynamics (e.g., incoherent tune shift).

The beam lifetime due to bremsstrahlung in the field of the ionic nuclei is given by [9]:

$$\frac{1}{\tau_{bs}} = - \sum_i \frac{16\lambda_{ion}r_e^2\alpha c Z_{a,i}^2}{6\pi\sigma_x\sigma_y} \log\left(\frac{\Delta E}{E}\right) \log\left(\frac{183}{Z_{a,i}^{1/3}}\right) \quad (8)$$

where the sum is over all atoms in a molecule, $Z_{a,i}$ is the charge of the nucleus of the i th atom (in units of the electron charge), A_a its mass (in units of the proton mass), α the fine structure constant, r_e the classical electron radius, σ_z and σ_y the rms beam size, and $\Delta E/E$ the energy acceptance of the ring. With $\Delta E/E \approx 0.01$ and assuming carbon monoxide, we find

$$\frac{1}{\tau_{bs}} \approx 3 \times 10^{-12} \lambda_{ion} \quad (9)$$

The lifetime can also be limited by single Coulomb scattering which dispels particles outside of the transverse acceptance. The cross section for this process is

$$\sigma_s = \frac{4\pi \sum_i Z_{a,i}^2 \alpha^2 \hbar^2}{q_{min}^2} \quad (10)$$

where $q_{min} = m_e c \gamma \sqrt{A_y / \beta_y}$ is the minimum transverse momentum transfer which leads to a particle loss (A_y is the vertical acceptance, which we take as $\gamma A_y \approx 200 \times 10^{-5}$ m, probably underestimating the actual acceptance which might be as large as 500×10^{-5} m). The beam lifetime due to single scattering is

$$\frac{1}{\tau_{ss}} \approx \frac{\sigma_s \lambda_{ion} c}{2\pi\sigma_x\sigma_y} \quad (11)$$

Inserting the above values, we obtain

$$\frac{1}{\tau_{ss}} \approx 1.5 \times 10^{-11} \lambda_{ion}, \quad (12)$$

which shows that, for the small acceptance assumed above, the single Coulomb scattering is five times more important than the bremsstrahlung.

In order to explain the observed beam lifetime of about 150 s by Coulomb scattering and bremsstrahlung, we would need an ion density of $\lambda_{ion} \approx 2 \times 10^8 \text{ m}^{-1}$, assuming that the volume density of neutral molecules is equal to the ion density. According to Fig. 7, we expect that an ion line density of this level is reached only during a time interval of 1–3 ms shortly after injection, whereafter the line density rapidly decreases to about $\lambda_{ion,\infty} \approx 2 \times 10^7 \text{ m}^{-1}$. For the latter value, the ring acceptance would have to be ten times smaller than assumed above in order to explain the reduced beam lifetime by Coulomb scattering. This is impossible.

Hence, the short lifetime must be attributed to either one (or both) of the two remaining, dynamical effects: collective ion-driven instabilities and/or perturbations of the single-particle dynamics by the ion space-charge field. This hypothesis is consistent with the observed strong tune dependence of the beam lifetime.

3 TUNE SHIFTS AND TRANSVERSE INSTABILITIES

3.1 Observations

From the ion-induced shift of the betatron tunes we can extract information about the ion species, density and dynamics. Many studies of the tune behavior were conducted using a stored beam. In order to generate a clear signal of the betatron motion, a noise or swept excitation was applied on a stripline kicker. Both the vertical and horizontal betatron tunes were observed as a function of time during the store, while the beam intensity gradually decayed. Figure 9 shows a typical tune measurement result for a single bunch. Depicted is the vertical betatron tune versus the beam intensity (in units of 10^{10} particles). At high current, the tune was fairly constant, but it started to shift monotonically upwards as the current dropped below about $N_{th} \approx 1.5 \times 10^{10}$. The total tune shift measured for a single bunch was of the order of $\Delta Q \approx 0.001$.

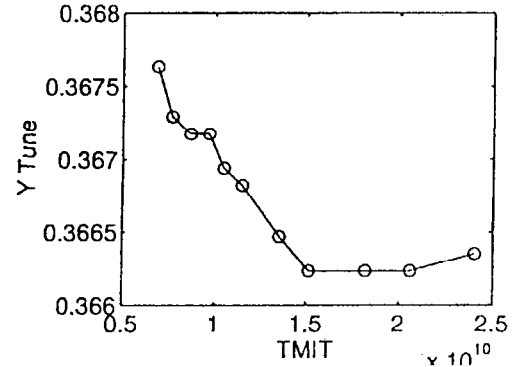


Figure 9: Fractional part of the vertical single-bunch betatron tune as a function of the bunch population (in units of 10^{10}), which was gradually decaying during the store.

When two bunches were stored in the ring, we observed spontaneous vertical and horizontal betatron sidebands. Strong coherent lines were seen for intensities between 1×10^{10} and 2.3×10^{10} particles per bunch (ppb). At lower currents the beam was stable (no sidebands present). For larger currents the beam was sometimes stable, but more often unstable. The self-excited sidebands are not observed under normal vacuum conditions, and were taken as evidence of an ion-induced transverse instability. These spontaneous lines appeared to be strongest around the odd-revolution harmonics, which would be suggestive of a coupled-bunch instability with π -mode character, where both bunches oscillate 180 degree out of phase. Another remarkable feature of the self-excited sidebands is that they extended over a very wide frequency range, up to 400 MHz. A typical spectrum is shown in Fig. 10.

For a betatron tune below the half integer resonance (0.44) and with two bunches stored, a sudden upward jump of the vertical tune by $\Delta Q_y = 0.022$ was observed, as the beam intensity decayed to about $N_b \approx 2 \times 10^{10}$ ppb. Prior to the jump the amplitude of the tune signal was large and

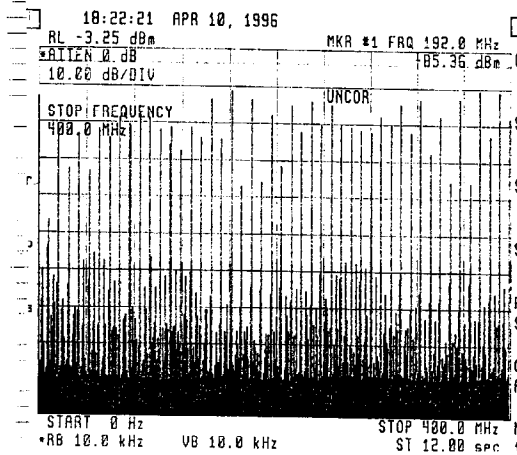


Figure 10: Bunch spectrum for 2 bunches with an intensity of $N_b = 4 \times 10^{10}$ each. A large number of self-excited vertical betatron sidebands are visible [6].

the frequency spread small, while after the jump the amplitude was small and the tune spread significantly widened (to a value of about 0.002). Figure 11 shows such an event, as recorded on the waterfall display of a Tektronix 3052 digital-signal-processing spectrum analyzer. The sudden tune jump was not observed for working points above the half-integer resonance.

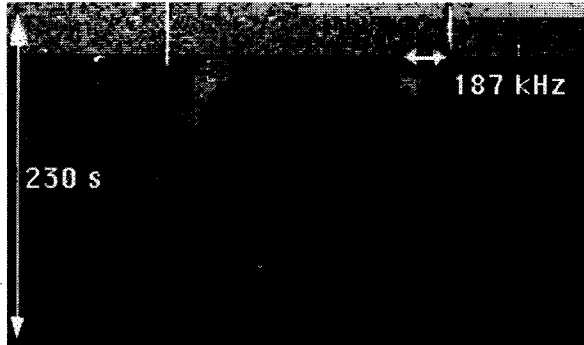


Figure 11: Evolution of self-excited vertical upper and lower betatron sidebands as a function of time after injection, with two bunches stored in the ring. The horizontal coordinate is the frequency (with a span of about 2 MHz), the vertical coordinate is the time (full scale is 230 s) which increases in the downward direction. The picture shows a sudden upward jump of the vertical betatron tune accompanied with a broadening of the tune line and a reduction of its amplitude.

We also measured the vertical beam size of the stored beam, using the image from a synchrotron light monitor. Figure 12 shows the vertical beam size along with the average bunch population of two stored bunches as a function of time, looking at two successive stores. The beam size (bottom picture) was large immediately after injection and also at low currents towards the end of the store. It was much smaller at intermediate intensities. Accidentally,

at these intermediate currents large spontaneous betatron lines were observed on the spectrum analyzer. So the small beam size and the self-excited betatron sidebands appeared to be well correlated. Unfortunately, due to lack of time this correlation has not been studied in more detail.

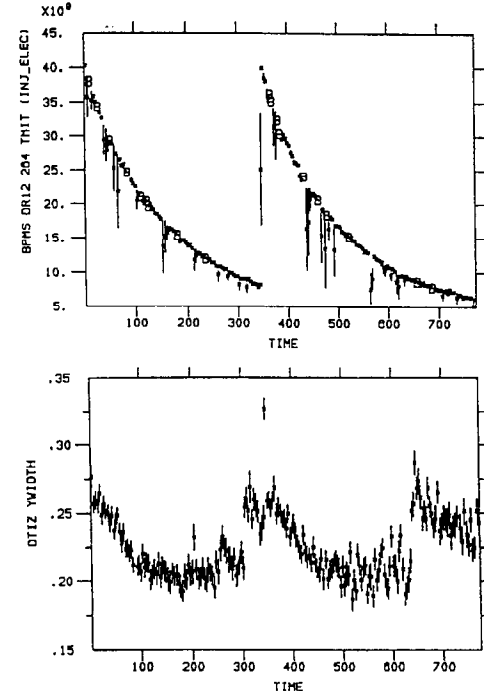


Figure 12: Bunch population in one of two bunches (top picture) and vertical beam size of the stored beam in arbitrary units (bottom picture) as a function of time (in seconds). Shown are two successive stores. The time intervals with increased vertical beam size at the beginning and end of a store coincided with periods where the beam appeared to be stable on the spectrum analyzer (no or only weak self-excited sidebands).

A transverse instability was not only observed when the beam was stored for seconds or minutes, but a much more violent instability was encountered during the first few milliseconds after injection. This transient instability probably was responsible for the large blow-up of the extracted beam emittance observed at the end of the regular 8.3-ms store. To study this transient instability, the spectrum analyzer was tuned to one of the excited sidebands and the frequency span was set to zero. Figure 13 shows two such measurements of the amplitude of the vertical betatron lower sideband $13f_0 - f_{\beta,y}$, where f_0 is the revolution frequency and $f_{\beta,y}$ the vertical betatron frequency. The tall peaks correspond to injection. After injection and damping of an initial oscillation, the amplitude suddenly increased with a submillisecond growth time, until a self-limiting amplitude was reached. Then the beam damped again. This process repeated itself irregularly several times during the 16.6-ms long store. Comparison of the top and bottom picture, taken on the same day under nominally identical con-

ditions, albeit at a slightly different frequency, exemplifies the irregularity of the instability. Often we observed 2 or 3 different instability patterns during the same injection cycle (e.g., compare the burst on the left in the upper figure or the burst on the right in the bottom picture with the remaining bursts). The varying patterns might correspond to different ion species becoming unstable at different times during the store.

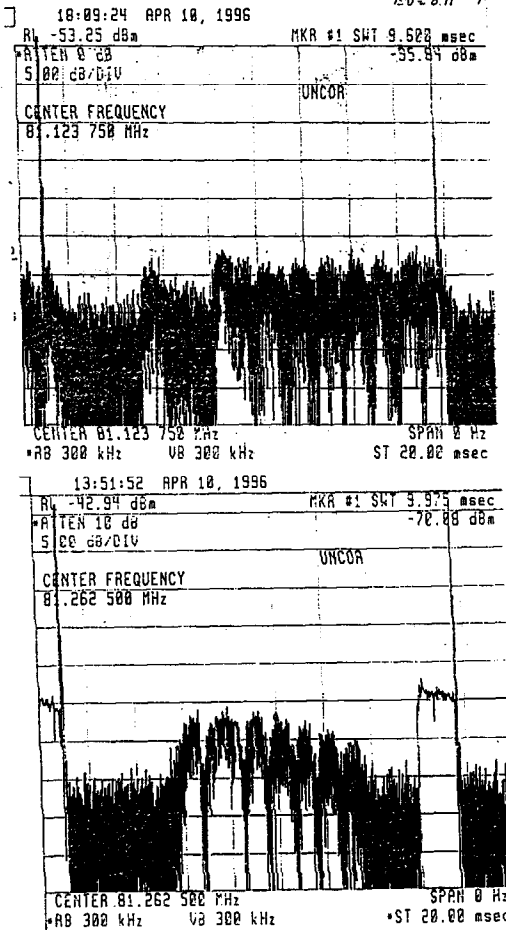


Figure 13: Time dependence of the amplitude of the $13f_0 - f_{\beta,y}$ vertical sideband during a 16.6-ms store. The tall peaks are the injection; the irregular bursts correspond to the instability [6]. We have no explanation for the smooth upward step about 2 ms before extraction in the bottom picture.

3.2 Theory

In the following three paragraphs, we compare and contrast the observations described in the previous section with theoretical expectations for the ion-induced tune shift, the ion oscillation frequency and the instability threshold.

3.2.1 Tune shift

Assuming that the distribution of the trapped ions is Gaussian with the same rms transverse dimensions as the beam,

the ion-induced coherent tune shift is given by

$$\Delta Q_{x,y} = \frac{r_e \beta_{x,y} \lambda_{ion} C Q}{\gamma 4 \pi \sigma_{x,y} (\sigma_x + \sigma_y)}, \quad (13)$$

which is independent of the ion mass. For an ion density equal to the residual-gas density, the ion-induced betatron tune shifts are about $\Delta Q_x \approx 0.003$ and $\Delta Q_y \approx 0.024$. Thus the expected vertical tune shift is very close to the tune jump of 0.022 observed on the waterfall display in Fig. 11!

3.2.2 Ion frequencies

The frequency at which a single ion oscillates in the average beam potential is given by

$$f_{ion, x,y} = \frac{c}{2\pi} \left(\frac{2N_{tot} r_p Q}{C \sigma_{x,y} (\sigma_x + \sigma_y) A} \right)^{1/2} \quad (14)$$

where $N_{tot} = n_b N_b$ is the total number of electrons in the beam and A the ion mass (in units of the proton mass). Figure 14 shows the horizontal and vertical ion frequencies, calculated from Eq. (14), as a function of time during the store, for two different ion species. A few milliseconds after injection, the ion frequencies extend up to 30 MHz for hydrogen and up to 10 MHz for carbon monoxide, respectively. These frequencies are much too low to explain the enormous frequency range of the self-excited betatron sidebands, shown in Fig. 10. One possible explanation is that, due to the nonlinearity of the beam-ion force, higher harmonics of the fundamental ion frequency are also excited.

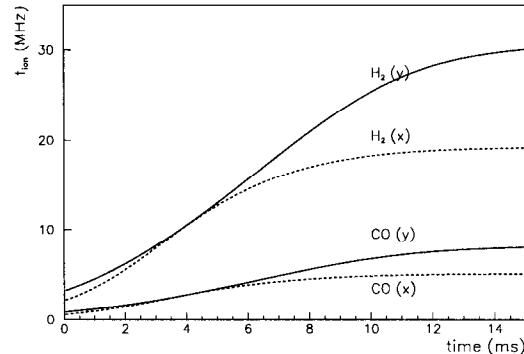


Figure 14: Predicted ion-oscillation frequency (in MHz) as a function of time during the store, for carbon monoxide ($A = 28$) and hydrogen ($A = 2$) ions.

3.2.3 Coherent instabilities

If an ion cloud interacts coherently with the beam, it can cause a collective instability. The classical theory of multi-turn beam-ion instabilities is discussed, for instance, in Ref.

[10, 11, 12]. To suppress the instability by Landau damping, the following condition must be satisfied [10, 11, 12]:

$$\Delta Q_y^{\text{rms}} \Delta Q_{\text{ion}}^{\text{rms}} \geq \left| \frac{Q_c^2 q}{Q_y} \right| \quad (15)$$

where ΔQ_y^{rms} denotes the rms betatron tune spread (e.g., caused by chromaticity and momentum spread or by the ion space-charge field), $\Delta Q_{\text{ion}}^{\text{rms}}$ the rms ion frequency spread (caused, e.g., by the variation of the beam sizes around the ring), Q_c the ion space-charge force on the electrons ($Q_c^2 = N_{\text{tot}}^{\text{ion}} r_e C Q / (2\pi^2 \sigma_y (\sigma_x + \sigma_y) \gamma)$), where $N_{\text{tot}}^{\text{ion}}$ denotes the total number of ions and Q the ion charge in units of e), q the electron beam space-charge force on the ions ($q = N_{\text{tot}} r_e C Q / (2\pi^2 \sigma_y (\sigma_x + \sigma_y) A)$), and Q_y the betatron tune. If we assume that the ion frequency spread is due to the beam-size variation around the ring, we can estimate that this spread is of the same magnitude as the ion frequency itself, $\Delta Q_{\text{ion}}^{\text{rms}} \approx q$. Since in reality the tune spread $\Delta Q_{\text{ion}}^{\text{rms}}$ is likely somewhat smaller than this, the threshold value for the rms vertical tune spread, ΔQ_y^{rms} calculated below, could be an underestimate.

Introducing the coherent tune shift due to the ions $\Delta Q_{\text{coh}} \approx Q_c^2 / (4Q_y)$, and using $Q_y \approx 3$, Eq. (15) predicts the instability threshold for $\Delta Q_y^{\text{rms}} \approx 4\Delta Q_{\text{coh}}$. As an example, if the coherent tune shift is $\Delta Q_{\text{coh}} \approx 0.025$, we expect that the instability is suppressed by Landau damping for tune spreads exceeding $\Delta Q_y^{\text{rms}} \geq 0.1$. The theory predicts that for a tune spread smaller than this, Landau damping is lost and the beam becomes unstable. Since typically measured tune spreads were much smaller (they were of the order of 0.002), the resulting Landau damping appears to be insufficient and an ion-induced instability is expected to occur. Unfortunately, it seems that the classical theory [10, 11, 12] does not explain why the instability disappeared at low current, where the measured tune spreads were still much too small to come even close to the theoretically predicted instability threshold.

An interesting observation is that the self-excited betatron sidebands, observed with two bunches that were stored for an extended period of time, were accompanied by a small vertical beam size and vice versa (see Fig. 12). A possible interpretation is the following. Both for the large initial beam sizes and for low current, the ions were stably trapped by the beam. These trapped ions caused a blow-up of the vertical beam size, perhaps via the (nonlinear) tune shift that they induced. For intermediate currents the ions were not stably trapped, but, at first sight surprisingly, they were not lost to the chamber wall either. Apparently, the ions interacted collectively with the beam, causing the observed transverse instability. We may speculate that due to the violent beam oscillations the average electric field around the beam orbit was reduced, thereby stabilizing the ion motion and allowing the ions to survive in the beam pipe. Since in this case the beam and the ions oscillated strongly with respect to each other, their spatial and temporal overlap was much smaller than in the case of stably trapped ions, and, thus, also the beam particles experienced

a much weaker average force from the ions. As a result, the beam size might have shrunk.

4 BEAM-TRANSFER-FUNCTIONS

4.1 Measurements

Further information about the beam-ion interaction can be obtained from the response of the beam to an external excitation. In such a beam-transfer-function measurement, the beam is harmonically driven at a frequency close to a betatron sideband, using a broadband transverse stripline kicker, and the beam response is measured on another stripline [7]. We used a conventional network analyzer to detect both the amplitude and the phase of the stored-beam response relative to the drive signal, as a function of the slowly swept excitation frequency. The data acquisition took several seconds, during which time the beam was stored in the ring. A schematic of the set-up is shown in Fig. 15. Since the coherent instability appeared to have a π -mode character, most measurements were conducted around the betatron sideband of an odd revolution harmonic.

The beam-transfer-functions measured with one and two bunches were strikingly different. While the single-bunch beam transfer function resembled that of a harmonic oscillator, the two-bunch response definitely did not. Most remarkable was that the phase of the two-bunch response did not suffer a net change but made a 90-degree excursion and then returned to its initial value as the excitation frequency crossed through the resonance. A detailed description of these measurements as well as a possible explanation can be found in Ref. [7].

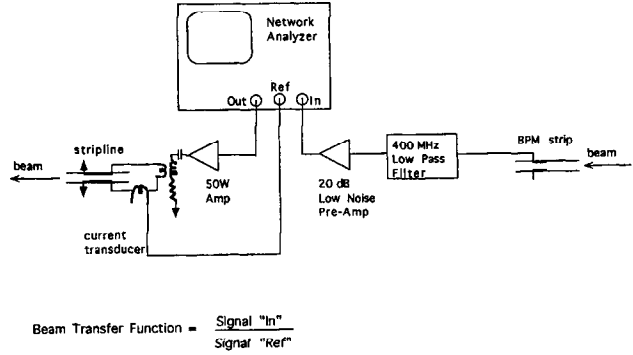


Figure 15: Schematic of set-up for transverse beam response measurement [7].

4.2 Interpretation

The difference in the single- and two-bunch responses appeared to be caused by the additional coupling of the two bunches which was introduced by the ions. Because the force between beam and ions is highly nonlinear, the two-bunch beam-transfer-function is qualitatively different

from that of a simple oscillator, and could be modeled by a higher-order response function [7]. In the case of a single bunch the effect of the ions on the beam-transfer-function was much smaller, the likely reason being that, when only one bunch is stored, the ions are dynamically unstable and most ions are quickly lost to the chamber wall.

Although an exact interpretation of the ion-dominated beam response is still missing, it appears that beam-transfer-function measurements provide a promising diagnostics for trapped ion effects in storage rings. In particular, the difference in the center frequencies of the σ and π -mode sidebands directly measures the strength of the linear bunch-to-bunch coupling due to the ions. If a period of poor vacuum should recur in future SLC runs, we plan to perform similar two-bunch beam-transfer-function measurements also around the sideband of an even revolution harmonic, in order to compare the response of the two eigenmodes in the ion-coupled system.

5 SUMMARY AND CONCLUSIONS

In 1996, unusually poor vacuum conditions in the SLC electron damping ring, with an average pressure around 10^{-7} Torr, resulted in significant ion production during the 8.3-ms beam store time. The current-dependent tune shift observed with a single bunch suggests a trapping threshold at an ion mass of about 45 amu (e.g. carbon dioxide). The ion-induced tune shift of about 0.02, detected with two bunches, is consistent with an ion density equal to the residual gas density, nicely confirming a postulation of Ref. [8] that the gas density represents an upper limit on the accumulated ion density!

The lifetime of the stored beam was a factor of ten worse than what could be explained by bremsstrahlung or Coulomb scattering on gas atoms and ions. The only conceivable explanation is that the bad lifetime was caused by ion-induced changes of the beam dynamics, either incoherent (e.g., nonlinear tune shift) or coherent (e.g., collective instability). A dynamical explanation is also supported by the observed strong dependence of the beam lifetime on the betatron tune.

It is interesting that the by far largest degradation of the beam quality occurred in the first few milliseconds after injection. Here, we observed a large emittance growth associated with a transverse instability in a parameter regime where ions could not be stably trapped by the beam. The emittance blow-up of the extracted beam, 8.3 ms after injection, was much larger for two bunches than for a single bunch, the instability being much stronger in the former case. The transverse instability in the first few milliseconds of the store is a good example of a transient ion effect, where the ions are trapped directly after injection when the beam sizes are large, while later, as the beam size shrinks and the ions become destabilized, they cause a coherent instability. Such transient ion effects could become important in many future fast-cycling machines, for example, in the damping rings of a next-generation linear collider [1].

Even when the beam was stored over extended periods of time, we still observed self-excited betatron sidebands, which were taken as evidence of a residual persistent instability. The sidebands disappeared when the current decreased to about 10^{10} particles per bunch. The observed tune shifts, tune spreads and instability threshold can (only) partly be explained by the classical theory of a two-stream instability, as developed in Refs. [10, 11, 12].

With a stored beam, we observed a spontaneous tune change when the vertical tune was set just below the half integer resonance (Fig. 11). Since for such tunes also the vertical beam size at the end of the 8.3-ms store time was relatively small (Fig. 5), a tune of about 3.42–3.45 was chosen as the nominal working point.

Finally, the measured two-bunch beam-transfer-function under poor vacuum conditions was very different from that of a harmonic oscillator and contains information about the nonlinear coupling of the two bunches due to the ions [7].

6 ACKNOWLEDGEMENTS

We thank Dr. S. Heifets for stimulating discussions and Prof. R. Siemann for his contributions to the beam observations. One of us (F.Z.) would like to thank Prof. S. Kurokawa, Dr. Y.-H. Chin and Dr. Y. Funakoshi for the invitation to this workshop and for financial support.

7 REFERENCES

- [1] This was pointed out by S. Heifets during the workshop.
- [2] R. Holtzapple, "Longitudinal Dynamics at the Stanford Linear Collider", Ph. D. thesis, SLAC-487 (1996).
- [3] C. Simopolous, R. Holtzapple, "Damping Rate Measurements in the SLC Damping Rings", IEEE PAC95, Dallas, p. 3073 (1995).
- [4] R.L. Holtzapple, R.H. Siemann, C. Simopoulos, "Measurements of Longitudinal Dynamics in the SLC Damping Rings", SLAC-PUB-95-6834, presented at PAC95 Dallas (1995).
- [5] T. Raubenheimer, F.J. Decker, J. Seeman, "Beam Distribution Function after Filamentation", SLAC-PUB-95-6850, presented at PAC95 Dallas (1995).
- [6] P. Krejcik, D. Pritzka, T. Raubenheimer, M. Ross, F. Zimmermann, "Ion Effects in the SLC Electron Damping Ring", SLAC-PUB-7546, presented at PAC97, Vancouver (1997).
- [7] P. Krejcik, "A Coupled Bunch Ion Instability in the SLC Electron Damping Ring", SLAC-PUB-7545, presented at PAC97, Vancouver (1997).
- [8] Y. Baconnier and G. Brianti, "The Stability of Ions in Bunched Beam Machines", CERN/SPS/80-2 (DI) (1980).
- [9] A. Piwinski, "Beam Losses and Lifetime", CERN 85-19 (1985).
- [10] G. Koshkarev and Zenkevich, Part. Acc. 3, "Resonance of Coupled Transverse Oscillations in Two Circular Beams", p. 1 (1972).
- [11] J.M. Laslett, A.M. Sessler, D. Möhl, "Transverse Two-Stream Instability in the Presence of Strong Species-Species

and Image Forces", Nuclear Instruments and Methods 121,
p. 517-524 (1974).

[12] R. Alves Pires et al., "On the Theory of Coherent Instabilities due to Coupling between a dense cooled Beam and charged Particles from the Residual Gas", Proc. of 1989 IEEE PAC, p. 800 (1989).